A Design for an EXIT Chart-Aided Adaptive Transmission Control Technique for Single-Carrier Based Multi-User MIMO Systems

Haruka Obata, Shinsuke Ibi and Seiichi Sampei
Department of Information and Communications Technology, Osaka University, Japan
Email: obata@wireless.comm.eng.osaka-u.ac.jp, {ibi, sampei}@comm.eng.osaka-u.ac.jp

***Abstract*— This paper proposes a scheduling and adaptive rate control scheme for multi-user multiple-input multiple-output (MIMO) systems in the uplink, designed to improve system throughput in single-carrier broadband wireless systems with a turbo equalizer. In the proposed scheme, to reduce computational burden for the scheduling and adaptive rate control, scheduling including stream selection is first conducted in the base station (BS) based on the expected signal to noise power ratio (SNR) after the turbo algorithm is converged. The BS also conducts coding rate optimization for each scheduled stream while convergence for the turbo equalizer is guaranteed thereby maximizing throughput efficiency. In order to guarantee the convergence property, this paper also proposes a rate control scheme suitable for the turbo equalization using an extrinsic information transfer (EXIT) trajectory which is predicted only from channel transfer functions. Computer simulation confirms that the achievable average system throughput can be significantly improved with the proposed scheme.**

I. Introduction

Demands for higher data rates and better quality in the uplink transmission of cellular broadband wireless systems have been increasing with the diversification of services. To satisfy these requirements, multi-user multiple-input multiple-output (MIMO) systems have attracted attention as one of the breakthroughs because of their potential improvements in terms of sum-rate capacity [1]. In such systems, an optimization of scheduling and rate control to determine *which user*, *which stream*, and *which rate* to transmit is a challenging problem, because residual inter-stream or inter-user interference limits achievable sum-rate capacity, which results in high computational complexity. Since exponential complexity increasing is unacceptable for practical systems, heuristic rules should be adopted to find a solution that achieves near-maximum sum-rate capacity.

In time-varying multi-user MIMO fading channels, each spatially multiplexed data stream may experience high channel gain at different timing. This phenomenon can be exploited to improve system throughput by scheduling radio resources with good conditions for each user. The improvement is widely known as a multi-user diversity effect [2], [3]. Furthermore, when the transmission rate is adaptively controlled according to the channel conditions at the assigned timing, redundancy in information rate can be reduced. The reduction is equivalent to minimization of a gap between channel capacity and a transmission rate.

In Ref. [3], one of the optimization methods has been proposed to achieve near-maximum sum-rate capacity with low complexity in spatial division multiplex access (SDMA) systems. However, with increased number of streams, the optimization's computational burden becomes heavy due to a greedy search procedure. On top of that, system throughput is not always improved although the theoretical sum-rate capacity is maximized. This is because a capacity-achieving data transmission scheme for any transmission rates is still an open issue. For the sake of the enhancement of system throughput, the adaptive rate control must take into account a fact that only *discrete* transmission rates are available in realistic transmission systems.

Recently, a frequency domain soft canceller with minimum mean square error (FD-SC/MMSE) turbo equalization has been recognized as one of the most promising techniques in applications of broadband mobile communications using single-carrier signaling [4]. To improve band-efficiency of the broadband single-carrier systems, Ref. [5] applies the MMSE turbo equalization technique to multilevel-bit interleaved coded modulation (ML-BICM) using higher-order modulations such as quadrature amplitude modulation (QAM) constructed by linearly weighted multiple binary sequences, by which the equalizer can separate the transmitted binary sequences constituting the QAM constellation.

Considering all of the above issues, this paper discusses the scheduling and rate control in the FD/SC-MMSE turbo-based multi-user MIMO system suitable for broadband single-carrier. The focus point of this paper is that the data streams from users can be perfectly discriminated, when an iterative detection of the FD/SC-MMSE turbo equalizer with ML-BICM signaling is successfully converged. This fact indicates that MIMO transmissions can be regarded as single-input multiple-output (SIMO) transmissions. Therefore, the base station (BS) needs not search all of the *combinations* of streams in the scheduling set to find out the optimal set that maximizes sum-rate capacity but just search a certain amount of SIMO streams in the descending order of achievable capacity in each stream. This feature suggests that the BS can appropriately schedule users with far low complexity. It is, however, required that the turbo

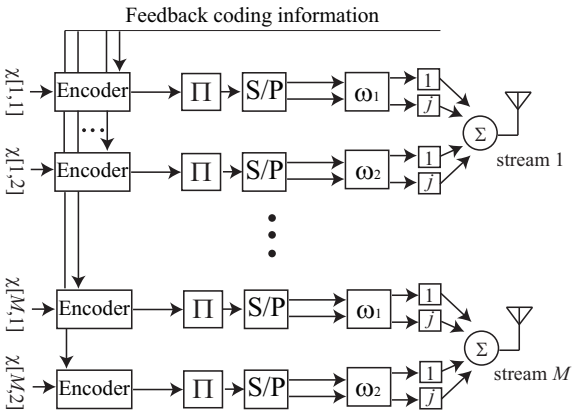

Fig. 1. Block diagram of the transmitter : Q=4

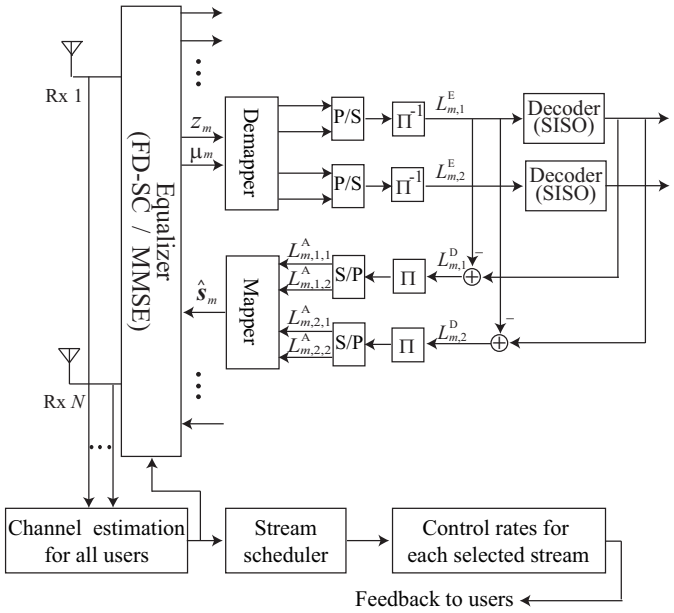

Fig. 2. Block diagram of the BS : Q=4

equalizer should be converged any time.

In fact, one of the rate control strategies used to converge the iterative detection in broadband single-carrier systems has been investigated in Ref. [5]. The strategy exploits an extrinsic information transfer (EXIT) property in the iterative turbo equalizer [6]. In detail, an EXIT trajectory depicted in previous consecutive frame transmission is used to allocate the optimal coding rate. However, the scheme cannot be directly applied to the scheduling process, because *a consecutive frame transmission is not always guaranteed*, thereby the trajectory for each spatially multiplexed stream cannot be always estimated using the trajectory analysis proposed in [5].

Fortunately, channel conditions, i.e. channel transfer functions, for the scheduled users can be measured in advance of the resource allocation when sharing-based channel state information (CSI) feedback channel is available. Therefore, this paper also proposes a simple EXIT property prediction scheme suitable for the rate control even in scheduling systems. There are two important points in the proposed scheme. The first one is that the starting and ending points of the trajectory are estimated only from the CSI feedback, and no knowledge on the iterative behavior is used. The second point is that the scheduled users are selected based only on the ending point of the trajectory to reduce computation burden, and the EXIT trajectory approximated by linear interpolation between at the starting and ending points is used to select the optimum coding rate (the highest coding rate while convergence of the turbo behavior is guaranteed) only for users to be scheduled in the next transmission. With this procedure, system throughput can be maximized with low computational burden in single-carrier broadband transmissions.

The rest of this paper is organized as follows: In Section II, the system model used in this paper is presented and the adaptive scheduling and rate control is described in Section III. The performance of the proposed scheme is evaluated in Section IV and followed by conclusions in Section V.

II. System Model

A. Multi User Environment

We consider a multi-user MIMO channel where a BS equipped with N receive (Rx) antennas can accommodate M streams in the uplink. The detailed channel model is described in Appendix. Note that U users with M_U streams resulting $UM_U > M$ streams are located in the environment and the M streams out of UM_U are selected by a criterion described in III-B at the BS.

B. ML-BICM Transmitter

Figure 1 shows a block diagram of a single-carrier based broadband MIMO transmitter with an adaptive rate control module. In this configuration, spectrum efficiency is flexibly controlled by ML-BICM [7] structure and high throughput can be supported by QAM constellation and MIMO transmission.

In the ML-BICM, each layer consists of a quaternary phase shift keying (QPSK) symbol sequence, and plural layers are weighted and superimposed to construct a higher level modulated symbol sequence. For example, when 2^Q ary QAM is employed, $Q/2$ layers of QPSK symbol sequence is superimposed. Therefore, when M streams are multiplexed in the MIMO system, the number of layers is $MQ/2$ in total [1]. Each layer is denoted as $\chi[m,q]$ $(m = 1, \cdots, M,\ q = 1, \cdots, Q/2)$. In the layer $\chi[m,q]$, the transmitted data sequence is encoded with a coding rate selected from the available code set, where a request of the selected coding rate in each layer is fed back from the receiver [9].

C. MMSE Turbo Receiver

Figure 2 shows a block diagram of the BS with an FD-SC/MMSE-based turbo equalizer which is used to mitigate

[1]Note that the terminology "layer" corresponds to the QPSK sequence although ML-BICM reported in Ref [8] is based on "level" of binary sequence.

inter-symbol, inter-channel and inter-layer interferences.

At the BS, the channel transfer functions for all users are estimated. After the received signal is converted into frequency domain by using a block-wise discrete Fourier transform (DFT) matrix, an expectation of a transmitted symbol $\underline{\hat{\boldsymbol{s}}}$ is calculated from decoder feedback [9]. Using $\underline{\hat{\boldsymbol{s}}}$, an interference residual vector is generated in a soft interference cancellation process, which is given by

$$\underline{\tilde{\boldsymbol{r}}} = \underline{\boldsymbol{r}} - \underline{\boldsymbol{H}}\underline{\hat{\boldsymbol{s}}}. \tag{1}$$

where

$$\underline{\hat{\boldsymbol{s}}} = [\hat{\boldsymbol{s}}_1^T, \cdots, \hat{\boldsymbol{s}}_m^T, \cdots, \hat{\boldsymbol{s}}_M^T]^T, \tag{2}$$

$$\hat{\boldsymbol{s}}_m = [\hat{s}_m(1), \cdots, \hat{s}_m(k), \cdots, \hat{s}_m(K)]^T, \tag{3}$$

where $\underline{\boldsymbol{r}}$ denotes the received signal, $\underline{\boldsymbol{H}}$ is channel matrix and K is the length of coded symbols to be transmitted.

The equalizer output vector $\boldsymbol{z}_m$ for the m-th stream can be derived by the frequency domain processing [10], [11], is given by

$$\boldsymbol{z}_m = (1+\gamma_m\delta_m)^{-1}[\gamma_m\hat{\boldsymbol{s}}_m + \boldsymbol{F}^H\boldsymbol{\Xi}_m^H\boldsymbol{\Psi}^{-1}\boldsymbol{F}_M\underline{\tilde{\boldsymbol{r}}}], \tag{4}$$

where

$$\begin{aligned}
\gamma_m &= \frac{1}{K}\mathrm{tr}[\boldsymbol{\Xi}_m^H\boldsymbol{\Psi}^{-1}\boldsymbol{\Xi}_m], && (5)\\
\boldsymbol{\Psi} &= \underline{\boldsymbol{\Xi}}\boldsymbol{\Delta}\underline{\boldsymbol{\Xi}} + 2\sigma^2\boldsymbol{I}_{NK}, && (6)\\
\boldsymbol{\Delta} &= (\boldsymbol{I}_M - \mathrm{diag}[\delta_1, \cdots, \delta_m, \cdots, \delta_M]) \otimes \boldsymbol{I}_K, && (7)\\
\delta_m &= \frac{1}{K}\sum_{k=1}^{K}|\hat{s}_m(k)|^2, && (8)
\end{aligned}$$

where $2\sigma^2$ is the noise spectral density, $\mathrm{tr}[\cdot]$ denotes a summation of diagonal elements in the matrix, $\mathrm{diag}[\cdot]$ denotes a matrix operator which extracts only diagonal elements in the matrix and $\underline{\boldsymbol{\Xi}}$ denotes the frequency domain representation of the channel matrix defined by

$$\underline{\boldsymbol{\Xi}} = [\boldsymbol{\Xi}_1, \cdots, \boldsymbol{\Xi}_m, \cdots, \boldsymbol{\Xi}_M]. \tag{9}$$

where $\boldsymbol{\Xi}_m$ is the frequency domain representation of the channel matrix among m-th stream and all Rx antennas pairs. The block-wise DFT matrix $\boldsymbol{F}_M$ is given by $\boldsymbol{F}_M = \boldsymbol{F} \otimes \boldsymbol{I}_M$ where $\boldsymbol{F}$ is a $K \times K$ DFT matrix, $\boldsymbol{I}_x$ is an $x \times x$ identity matrix and $\otimes$ denotes Kronecker product.

Let us assume that the equalizer output follows a Gaussian distribution [12], the equalizer output can be approximated as [8], [9]

$$\boldsymbol{z}_m = \mu_m\boldsymbol{s}_m + \psi, \tag{10}$$

where μ_m, $\boldsymbol{s}_m$ and ψ represents equivalent amplitude level, transmit signal from the m-th stream and zero mean independent complex Gaussian noise with variance N_m, respectively. From Eqs. (4) and (10), the gain μ_m, the complex variance N_m and signal to noise power ratio (SNR) snr_m of the equalizer output for the m-th stream can be expressed as

$$\begin{aligned}
\mu_m &= (1+\gamma_m\delta_m)^{-1}\gamma_m, && (11)\\
N_m &= \mu_m - \mu_m^2, && (12)\\
snr_m &= \frac{(\mu_m)^2}{N_m}. && (13)
\end{aligned}$$

After calculation of extrinsic log likelihood ratios (LLRs) based on the equalizer output at a demapper and Eqs. (11) and (12) [7], a parallel-to-serial (P/S) converter provides LLR stream for each layer $L_{m,q}^E$. The obtained LLR $L_{m,q}^E$ is forwarded to the soft-input soft-output (SISO) decoders followed by calculation of the decoder output LLR $L_{m,q}^D$. After $L_{m,q}^D$ is interleaved and S/P converted, the expected transmitted symbol $\hat{\boldsymbol{s}}_m$ is generated. These extrinsic LLRs for the q-th layer of m-th stream are iteratively exchanged between the equalizer and the decoders via deinterleaver and interleaver.

III. Adaptive Scheduling and Rate Control

A. Convergence Property on an EXIT Chart

According to Ref. [5], [6], the mutual information (MI) I between the transmitted coded bits $\mathcal{C} \in \{\pm 1\}$ with equiprobable occurrence and the extrinsic LLR is given by

$$\begin{aligned}
I &= 1 - \int_{-\infty}^{\infty} p_{L|\mathcal{C}}(\xi|+1)\log_2(1+e^{-\xi})d\xi \\
&= 1 - \frac{2}{K}\sum_{k=1}^{K}\frac{\log_2(1+e^{-L_k})}{1+e^{-L_k}} && (14)
\end{aligned}$$

where $p_{L|\mathcal{C}}(\xi|b)$ is a probability density function (PDF) of LLR being ξ conditioned upon the coded bit b, and L_k is the LLR of the k-th bit. Eq. (14) indicates that the extrinsic LLR stream for the equalizer output ($L_{m,q}^E$) and that for the decoder output ($L_{m,q}^D$) can be easily transformed into MI for the equalizer output ($I_{m,q}^E$) and that for the decoder output ($I_{m,q}^D$), respectively.

1) Decoder EXIT Function: A decoder EXIT function for a convolutional code with an arbitrary code structure is uniquely defined by

$$I_{m,q}^D = G_R(I_{m,q}^E). \tag{15}$$

Figure 3 shows the EXIT characteristics of several channel decoder outputs for convolutional codes with its constraint length of four specified by Ref. [13]. The decoder EXIT curves in this figure are for a set of coding rates $\mathcal{R}$ from $1/8$ to $7/8$, as described in the figure caption. Curves with higher coding rate are located higher.

2) Equalizer EXIT Function: Despite the ease in calculation of the MI for the equalizer output, analyzing the EXIT characteristic of each layer with $M > 1$ or $Q > 2$ is not easy, because a certain layer's MI transfer function depends on the other streams' and layers' decoder output MI, which is formulated as

$$\begin{aligned}
I_{m,q}^E = F_{m,q}\,(&I_{1,1}^D, \cdots, I_{1,Q/2}^D, \cdots, I_{m,1}^D, \cdots, I_{m,Q/2}^D, \\
&\cdots, I_{M,1}^D, \cdots, I_{M,Q/2}^D, \underline{\boldsymbol{\Xi}}, E_s/N_0). \quad (16)
\end{aligned}$$

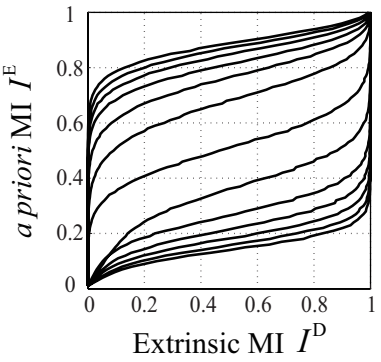

Fig. 3. Decoder EXIT curves for $\mathcal{R}$=7/8, 6/7, 5/6, 4/5, 3/4, 2/3, 1/2, 1/3, 1/4, 1/5, 1/6, 1/7, *and* 1/8 from top to down

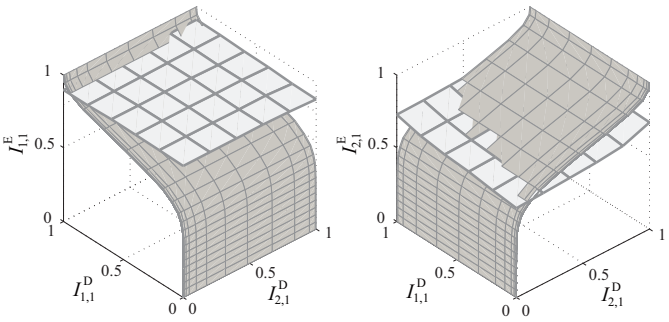

Fig. 4. Multi-dimensional EXIT chart

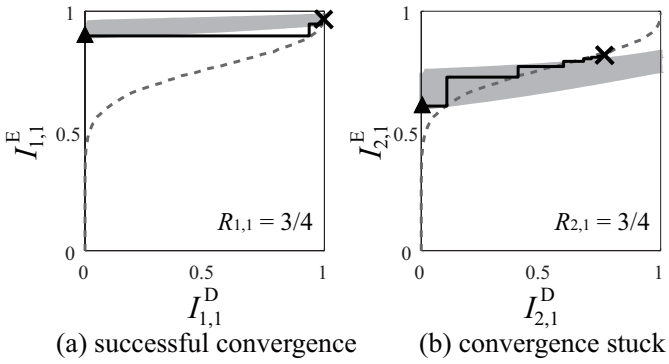

Fig. 5. Projected EXIT chart of Fig. 4: (a) codes with R = 3/4 (b) codes with R = 3/4.

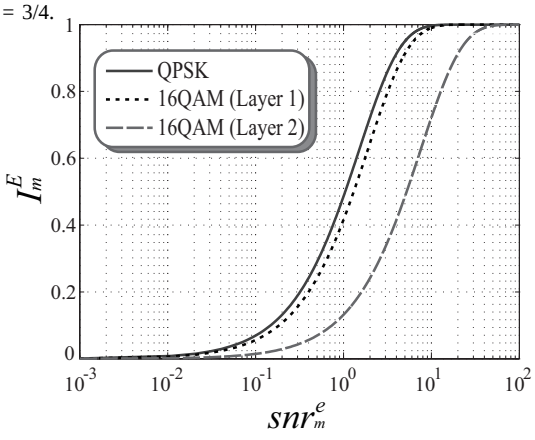

Fig. 6. Equalizer output MI $I^{E}_{m,q}$ versus snr^{e}_{m}

where E_s/N_0 is energy-per-symbol to the noise spectral density.

3) EXIT Chart: A snapshot of the EXIT chart for a layer and a stream is depicted in Fig 4, where $M = 2$, $N = 2$, $Q = 2$ (QPSK), 24-path frequency selective fading with 2 dB exponential decay factor, and E_s/N_0 = 6 dB. The MI is calculated by 4096 coded bit length. In this case, since each MI depends on feedback MI from the both decoders of the two streams, the EXIT characteristic is expressed by planes. When the number of streams and layers increases more, the EXIT chart becomes multi-dimensional, which is impossible to be visualized.

However, convergence analyses for $M > 1$ or $Q > 2$ can be accommodated by projecting the EXIT functions onto two dimensional planes constructed by the equalizer output MI and one of the decoder's output MI [14]. Figure 5 shows projected EXIT chart of Fig. 4. Gray zones represent region of the equalizer output MI $I^{E}_{m,q}$ at an arbitrary value of $I^{D}_{m,q}$. In other words, the lower bound corresponds to the case when the decoder output MI values fed back from the other stream are zero, and the upper bound corresponds to the case when those are one. Solid lines in Fig. 5 show the projected trajectories which demonstrate a behavior of iterative detection process. The key point of the iterative process is that the symbol stream is correctly detected only if the trajectory reaches $I^{D}_{m,q} \approx 1$ as shown in Fig. 5 (a). In this paper, this situation is called as "The trajectory is converged." In contrast, the detection is failed if the trajectory is stuck at the point where $I^{D}_{m,q} < 1$, as shown in Fig. 5 (b). With the same manner, behavior of iterative detection process in the case of more streams or layers can be visualized.

B. Scheduling

We now consider that there are U users with M_U streams resulting $UM_U(> M)$ streams in the environment, and the BS selects M streams out of UM_U streams. The M data streams are independently detected, when the iterative detection of the FD/SC-MMSE turbo equalizer is successfully converged – corresponding to successful cancellation of inter-symbol, inter-channel and inter-layer interferences –. If the turbo equalizer is converged, since perfect knowledge about transmitted symbol is obtained from decoder feedback information, δ_m becomes 1 for all m. Therefore, the gain μ^{e}_{m}, the complex variance N^{e}_{m} and SNR snr^{e}_{m} of the equalizer output for m-th stream given by Eqs.(11)-(13) at the ending point can be rewritten as

$$\mu^{e}_{m} = (1+\gamma^{e}_{m})^{-1}\gamma^{e}_{m}, \quad (17)$$

$$N^{e}_{m} = \mu^{e}_{m} - (\mu^{e}_{m})^{2}, \quad (18)$$

$$snr^{e}_{m} = \frac{(\mu^{e}_{m})^{2}}{N^{e}_{m}} = \gamma^{e}_{m}, \quad (19)$$

where γ^{e}_{m} is given by

$$\gamma^{e}_{m} = \frac{1}{2\sigma^{2}_{\nu}K}\mathrm{tr}\,[\mathbf{\Xi}^{H}_{m}\mathbf{\Xi}_{m}]. \quad (20)$$

According to Eqs.(17)-(20), MIMO transmissions can be regarded as SIMO transmissions because the equalizer outputs are independent of each stream. This feature indicates the decoder output for each stream is uniquely determined without impacts on combination of simultaneously transmitted stream, when the equalizer is successfully converged.

In addition, as long as the equalizer output can be regarded to be subject to a Gaussian random process, the equalizer output MI $I_{m,q}^E$ can be approximately given by the J function [14] for each layer as

$$I_{m,q}^E = J(\sigma_m^e) \approx \left(1 - 2^{-H_1(\sigma_m^{e2})^{H_2}}\right)^{H_3} \quad (21)$$

where the parameter σ_m^e is defined as

$$\sigma_m^{e2} = \begin{cases} 4snr_m^e & (Q=2) \\ 3.2snr_m^e & (Q=4, \text{Layer1}) \\ 0.8snr_m^e & (Q=4, \text{Layer2}), \end{cases} \quad (22)$$

and relationship between I_m^E and snr_m^e are shown in Figure 6. The mapping-specific parameters are $H_1 = 0.3073$, $H_2 = 0.8935$ and $H_3 = 1.1064$ that are obtained by least-squared curve fitting [15]. Note that the approximation approach has been originally proposed by Brannstrom [14]. According to Fig. 6, the J function is a monotonically increasing function.

This independency involved in calculation of MI suggests that the BS should select M streams for simultaneous transmission out of UM_U based on following rule:

1. Calculate $snr_{m'}^e(m' = 1, ..., UM_u)$ for all UM_U stream candidates where $\mathbf{\Xi}_{m'}$ for each stream candidate is perfectly known at the BS.
2. Select top M streams having higher $snr_{m'}^e$ among UM_U stream candidates.

As a result, user and stream selection process in the scheduling is extremely simplified compared to the previously proposed searching algorithms [3]; just to choose user and stream having higher $snr_{m'}^e$.

As explained before, the EXIT trajectory is useful for the evaluation of the convergence [5], and it is applicable if data streams are consecutively transmitted. However, in the scheduling process, a consecutive frame transmission is not always guaranteed, which means that the equalizer output MI for each stream cannot always be estimated using trajectory analysis for previously transmitted signals. In the broadband wireless access systems, fortunately, we usually have some means to evaluate channel transfer function. Thus, this paper proposes an adaptive rate control scheme for *selected* users using EXIT trajectories predicted only from channel transfer functions without any information about EXIT trajectories of previous transmissions in next subsection.

C. Rate Control

In order to predict the trajectory behavior, we now focus on a starting point and an ending point on the EXIT charts. The ending point can be calculated by Eq. (21). On the other hand, the starting point is determined by the equalizer output at the first iteration [9]. At this stage, feedback information from the decoder does not exist, i.e., δ_m is 0. Therefore, the gain μ_m^s, the complex variance N_m^s and SNR snr_m^s of the equalizer output for the m-th stream of Eqs.(11)-(13) at the starting point can be rewritten as

$$\mu_m^s = \gamma_m^s, \quad (23)$$

$$N_m^s = \mu_m^s - (\mu_m^s)^2, \quad (24)$$

$$snr_m^s = \frac{(\mu_m^s)^2}{N_m^s} = \frac{\gamma_m^s}{1-\gamma_m^s}, \quad (25)$$

where γ_m^s is given by

$$\gamma_m^s = \frac{1}{K}\text{tr}\left[\mathbf{\Xi}_m^H \left(\underline{\underline{\mathbf{\Xi}\mathbf{\Xi}}}^H + 2\sigma_\nu^2 \mathbf{I}_{NK}\right)^{-1} \mathbf{\Xi}_m\right]. \quad (26)$$

Invoking a Gaussian channel assumption again, the starting point is approximated by least-squared curve fitting [15] expressed as

$$I_{m,q}^E = J_q(snr_m^s) \approx \left(H_1 - H_2^{-H_3(snr_m^s)^{H_4}}\right)^{H_5}, \quad (27)$$

where the mapping-specific parameters H_1, H_2, H_3 H_4 and H_5 for each layer are listed in Table I. Therefore, the starting and ending points are constructed only from SNR of the equalizer output depending on the channel transfer functions.

TABLE I
APPROXIMATION PARAMETERS FOR EQ. (27)

Layer	H_1	H_2	H_3	H_4	H_5
1	1.0045	0.4805	-2.2073	0.3187	4.7618
2	1.0027	1.4166	0.1675	1.1746	0.9966

We now consider to approximate the trajectory for each layer with a straight line connected between the starting and ending points. In order to assess the code optimality in terms of the convergence property, examples of the equalizer and the decoder output MI transfer characteristics under a given channel realization are depicted in Figure 7, where $M = 2$, $N = 2$, $Q = 4$ (16QAM), $E_s/N_0 = 15$ dB, 24-path frequency selective fading with an exponential decay factor 2 dB, and 4096 coded bits length are assumed. The trajectories of the MI exchange until eighth iteration are plotted in the figures. There are four trajectories corresponding to the layers $\chi[1,1]$, $\chi[1,2]$, $\chi[2,1]$, $\chi[2,2]$. Fig. 7 (a) shows the case when all layers can select coding rate without including large redundancy. As can be seen in the figures, the approximated solid line matches well with the trajectories of MI exchange, which correspondence suggests that we can guarantee convergence with a high probability using the approximated solid line.

However, there might be actually a case where transmissions cannot successfully converge although the approximated solid line does not intersect with a corresponding decoder EXIT curve as shown in the Fig. 7 (b) due to lack of iterations. Therefore, we add a simple criterion to guarantee the convergence by setting a window between the approximated solid line and the corresponding decoder EXIT curve as shown in Figure 8. The approximated solid line and the corresponding decoder EXIT curve are always separated with window size w or more. With this criterion, it is expected that transmissions

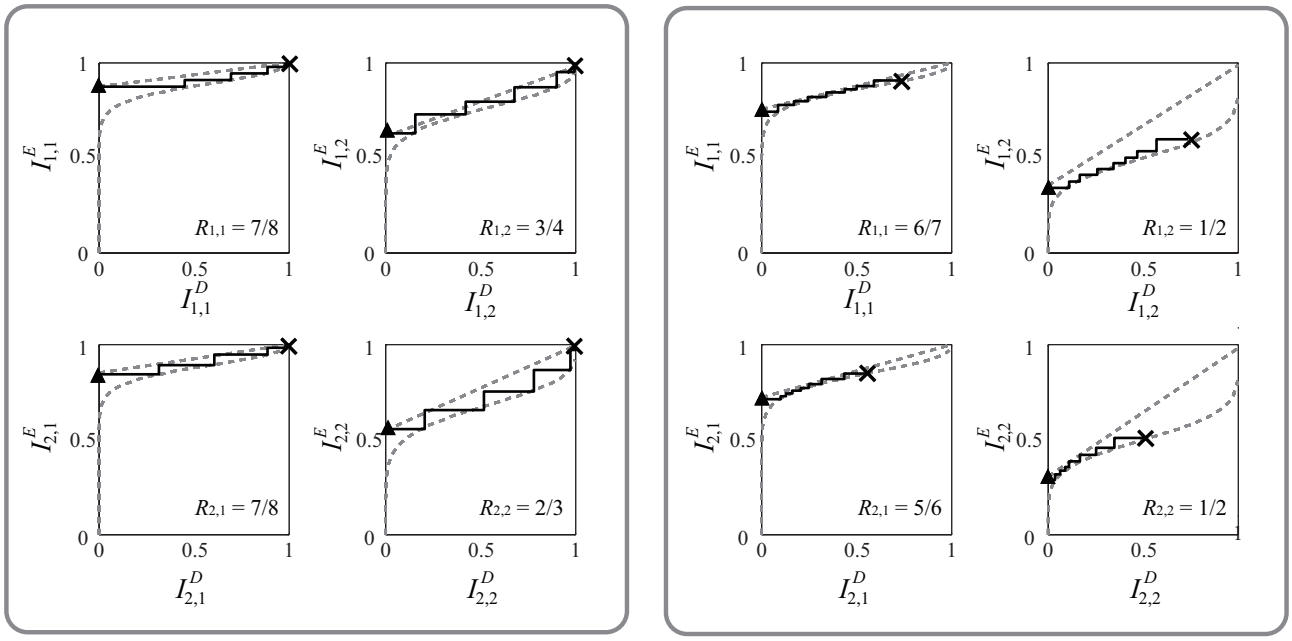

(a) successful convergence (b) convergence stuck

Fig. 7. Snapshots of trajectories in iterative decoding

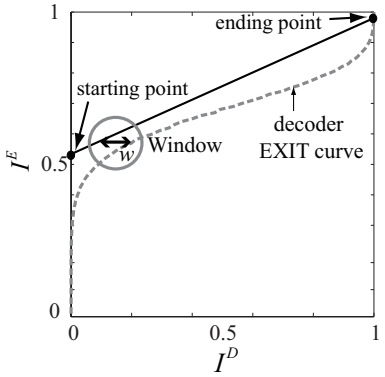

Fig. 8. Concept of window control

TABLE II

AN EXAMPLE OF THE PRE-CALCULATED $\eta^{\alpha}_{\mathcal{R}}$

$\mathcal{R}$	1/8	1/7	1/6	1/5	1/4
$\eta^{\alpha}_{\mathcal{R}}$	0.3183	0.3567	0.4040	0.4701	0.5545
$\mathcal{R}$	1/3	1/2	2/3	3/4	4/5
$\eta^{\alpha}_{\mathcal{R}}$	0.6602	0.8197	0.9256	0.9509	0.9618
$\mathcal{R}$	5/6	6/7	7/8		
$\eta^{\alpha}_{\mathcal{R}}$	0.9714	0.9825	0.9848		

successfully converge at any time, even in the number of iterations is limited.

This convergence feature suggests that the BS should select a coding rate for each layer at the m-th stream based on the following rule:

1. To achieve high coding rate, select a set $\mathcal{R}$ of coding rates of which satisfying $\eta^{\alpha}_{\mathcal{R}} < I^{E(end)}_{m,q}$ namely
$$\mathcal{C} \in \{\mathcal{R} \,|\, \eta^{\alpha}_{R} < I^{E(end)}_{m,q}\} \tag{28}$$
for each rate in the set of rates $\mathcal{R}$, where η^{α}_{R} denotes the equalizer output MI required to yield frame error rate (FER) $\leq \alpha$ [9]. An example of the pre-calculated η^{α}_{R} values at $\alpha = 0.1$ for the convolutional codes are listed in Table II.
2. One step lower coding rate is selected if the convergence property applying the concept of window-control is not guaranteed.

IV. COMPUTER SIMULATION

A. Simulation Parameters

Computer simulation has been conducted to verify an enhancement of throughput efficiency by the proposed system. Table III specifies the main simulation parameters. In this simulation, there are four users and each user can transmit up to two streams. At the BS, four Rx antennas are equipped to discriminate up to four streams at the receiver. Thus, four streams among potential eight stream candidates are scheduled and rates are controlled to maximize the throughput efficiency. As for the channel state, the same average path loss including shadowing is assumed for all users, and only uncorrelated instantaneous frequency-selective fading is assumed for each stream, where 24-path Rayleigh-fading channel with an average path energy having a decaying factor of 2 dB between the consecutive paths is assumed. 16QAM ML-BICM is employed and coding rate for each layer is independently controlled according to the algorithm explained in Sect. III-C. The Max-Log-Maximum *a-posteriori* probability (MAP) algorithm with

TABLE III
SIMULATION PARAMETERS

Modulation rate	Multilevel 16QAM BICM
Coding rate	7/8, 6/7, 5/6, 4/5, 3/4, 2/3, 1/2, 1/3, 1/4, 1/5, 1/6, 1/7,1/8
Data symbol length	2048 symbols
Cyclic prefix	64 symbols
Channel coding	non-systematic convolutional code (constraint length 4)
Decoder	Max-Log-MAP with Jacobian logarithm
Interleaver	Random
Number of Rx antennas	4
Number of transmit stream for each user	2
Number of users	4
Number of selected streams	4
Channel model Delay profile	24-path Rayleigh fading exponentially 2 dB decaying
Channel estimation	Perfect

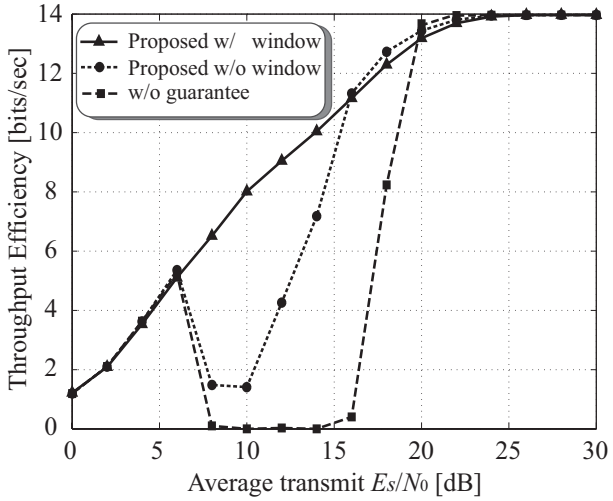

Fig. 9. Average throughput versus transmit E_s/N_0 property with adaptive coding

Jacobian logarithm is used in the each layer's SISO decoder [16] and the number of iteration in the turbo algorithm is set to eight. The estimation of channel states and the notification of the selected coding parameters are assumed to be perfect.

B. Simulation Results

Figure 9 shows throughput efficiency of the proposed scheduling and rate control scheme with and without the window control. In addition, the performance without a guarantee function of the trajectory convergence (coding rate is selected only by Eq. (28)) is also shown in the figure as a reference curve. Note that throughput efficiency is defined as [*summation of number of source bits in successful received frames*] / [*transmitted time duration in unit of symbol duration*], and transmit E_s denotes an transmit energy-per-symbol.

The performance of the non-guaranteed convergence scheme selects a code for each layer in the set $\mathcal{R}$ of coding rates of which rate satisfying $\eta_{\mathcal{R}}^{\alpha} < I_{m,q}^{E(end)}$ so that the coding rates are determined by FER requirement $\alpha = 0.1$ [9]. It is found from the figure that there is a "valley" around $E_s/N_0 = 10$ dB. This is because the equalizer EXIT curve intersects with the corresponding decoder EXIT curve before achieving the target MI, thereby resulting in frame errors.

The performance of the proposed scheme without window also faces to the same "valley" phenomenon around $E_s/N_0 = 10$ dB. This is because the convergence of the trajectory cannot always be guaranteed due to the lack of iterations even when the equalizer EXIT curve does not intersect with the selected decoder EXIT curve before achieving the target MI.

On the other hand, the performance of the proposed scheme with the window size $w = 0.1$ can improve throughput efficiency with E_s/N_0 without an event of "valley". The value $w = 0.1$ is optimized in the given simulation conditions. However, the optimum value is almost identical in other conditions.

These results confirm that the proposed EXIT chart aided scheduling and rate control technique with the window control is effective in properly enhance system throughput with increasing E_s/N_0.

V. CONCLUSION

An efficient EXIT chart aided scheduling and adaptive rate control scheme for multi-user broadband MIMO systems has been proposed in this paper. The proposed scheduling and rate control scheme provides high data throughput in time varying spatio-temporal channel characteristics with low complexity. Computer simulation confirms that the throughput efficiency can be improved with E_s/N_0 using the proposed scheme.

ACKNOWLEDGMENT

The authors would like to thank Prof. Tad Matsumoto with Japan Advanced Institute of Science and Technology, Japan, and Centre for Wireless Communications, University of Oulu, Finland for valuable comments and suggestions. This research was supported in part by "Global COE (Centers of Excellence) Program" of the Ministry of Education, Culture, Sports, Science and Technology, Japan.

REFERENCES

[1] M. H. V. Stankovic, "Improved diversity on the uplink of multi-user mimo systems," in *Proc ECWT '05*, vol. 3-4, Paris, France, Oct. 2005, pp. 113 – 116.

[2] M. Z. W. A.F.Molisch and J.H.Winters, "Capacity of MIMO systems with antenna selection," in *Proc. ICC '01*, vol. 2, Helsinki, Finland, June 2001, pp. 570–574.

[3] R. Zhang, "Scheduling for maximum capacity in SDMA/TDMA networks," in *Proc. ICASSP'02*, vol. 3, Orlando, Fla, USA, May 2002, pp. 2141–2144.

[4] D. Reynolds and X. Wang, "Low complexity turbo-equalization for diversity channels," *Signal Processing, Elsevier Science Publishers*, vol. 81, no. 5, pp. 989–995, May 2001.

[5] S. Ibi, T. .Matsumoto, S. Sampei, and N. Morinaga, "EXIT chart-aided adaptive coding for MMSE turbo equalization with multilevel BICM," *IEEE Communications Letters*, vol. 10, pp. 486–488, 2006.

[6] S. ten Brink, "Convergence behavior of iteratively decoded parallel concatenated codes," *IEEE Trans. Commun.*, vol. 49, no. 10, pp. 1727–1737, Oct. 2001.

[7] A. Dejonghe and L. Vandendorpe, "Turbo-equalization for multilevel modulation: an effcient low-complexity scheme," in *Proc. ICC '02*, vol. 3, New York, USA, Apr. 28-May 2 2002, pp. 1863–1867.

[8] K. Kansanen and T. Matsumoto, "An analytical method for MMSE MIMO turbo equalizer EXIT chart computation," *IEEE Trans. Wireless Commun.*, vol. 6, no. 1, pp. 59–63, Jan. 2007.
[9] S. Ibi, T. Matsumoto, S. Sampei, and N. Morinaga, "EXIT chart-aided adaptive coding for multilevel bicm with turbo equalization in frequency selective mimo channels," *to be published*.
[10] M. Tüchler and J. Hagenauer, "Turbo equalization using frequency domain equalizers," in *Proc. Allerton Conf.*, Monticello, IL, USA, Oct. 2000, pp. 1234–1243.
[11] K. Kansanen, "Wireless broadband single-carrier systems with MMSE turbo equalization receivers," Ph.D. dissertation, University of Oulu, Dec. 2005.
[12] H. Poor and S. Verdu, "Probability of error in MMSE multiuser detection," *IEEE Trans. Inform. Theory*, vol. 43, no. 3, pp. 858–871, May 1997.
[13] J. G. Proakis, *Digital Communications*, 4th ed. New York: McGraw-Hill, 2001.
[14] F. Brannstrom, "Convergence analysis and design of multiple concatenated codes," Ph.D. dissertation, Chalmers University of Technology, 2004.
[15] J. A. Nelder and R. Mead, "A simplex method for function minimization," *Computer Journal*, vol. 7, pp. 308–313, 1965.
[16] P. Robertson, E. Villebrun, and P. Hoeher, "A comparison of optimal and sub-optimal MAP decoding algorithms operating in the log domain," in *Proc. ICC*, Seattle, USA, June 1995, pp. 1009–1013.

APPENDIX

multi-user MIMO channel

In this paper we consider multi-user MIMO channels where a BS equipped with N receive (Rx) antennas can accommodate M streams simultaneously.

A symbol transmitted at a discrete time k from the m-th stream is denoted by $s_m(k)$. The channel impulse response (CIR) between the m-th stream and the n-th Rx antenna, is denoted by $h_{n,m}(t = lT_s) = h_{n,m}(l)$ with T_s being a symbol duration. The received symbol $r_n(k)$ received at the n-th Rx antenna can be expressed by the convolution of the transmit signal and the CIR as

$$r_n(k) = \sum_{l=0}^{L-1} \sum_{m=1}^{M} h_{n,m}(l) s_m(k-l) + \nu_n(k), \tag{29}$$

where L denotes the channel memory length, and $\nu_n(k)$ denotes zero mean additive white Gaussian noise sample with variance $2\sigma^2$.

To apply a frequency domain processing with low computational complexity at the receiver, a length P symbol cyclic prefix (CP) is added to each transmitted symbol stream, resulting the total transmitted symbol block length becomes $P + K$. Removing the CP at the receiver, the channel model in a matrix form is expressed as

$$\underline{\boldsymbol{r}} = \underline{\boldsymbol{H}}\,\underline{\boldsymbol{s}} + \underline{\boldsymbol{\nu}} \tag{30}$$

where $\underline{\boldsymbol{r}}$, $\underline{\boldsymbol{s}}$, and $\underline{\boldsymbol{\nu}}$ are the received signal, the transmitted signal, and the Gaussian noise vectors, respectively, and they are given by

$$\underline{\boldsymbol{r}} = \left[\boldsymbol{r}_1^T, \cdots, \boldsymbol{r}_n^T, \cdots, \boldsymbol{r}_N^T\right]^T, \tag{31}$$

$$\underline{\boldsymbol{s}} = \left[\boldsymbol{s}_1^T, \cdots, \boldsymbol{s}_m^T, \cdots, \boldsymbol{s}_M^T\right]^T, \tag{32}$$

and

$$\underline{\boldsymbol{\nu}} = \left[\boldsymbol{\nu}_1^T, \cdots, \boldsymbol{\nu}_n^T, \cdots, \boldsymbol{\nu}_N^T\right]^T \tag{33}$$

with their component vectors being

$$\boldsymbol{r}_n = [r_n(1), \cdots, r_n(k), \cdots, r_n(K)]^T, \tag{34}$$

$$\boldsymbol{s}_m = [s_m(1), \cdots, s_m(k), \cdots, s_m(K)]^T, \tag{35}$$

and

$$\boldsymbol{\nu}_n = [\nu_n(1), \cdots, \nu_n(k), \cdots, \nu_n(K)]^T. \tag{36}$$

With definitions of the terms above, the channel matrix can then be defined as

$$\underline{\boldsymbol{H}} = [\boldsymbol{H}_1, \cdots, \boldsymbol{H}_m, \cdots, \boldsymbol{H}_M] \tag{37}$$

with its component sub-matrices being

$$\boldsymbol{H}_m = \left[\boldsymbol{H}_{1,m}^T, \cdots, \boldsymbol{H}_{n,m}^T, \cdots, \boldsymbol{H}_{N,m}^T\right]^T, \tag{38}$$

where $\boldsymbol{H}_{n,m}$ is a circulant-matrix based on the column vector $[h_{n,m}(0), \cdots, h_{n,m}(L-1), \mathbf{0}_{K-L}]^T$ and $\mathbf{0}_x$ denotes an all-zeros vector with length x.

The frequency domain representation of the channel matrix $\underline{\boldsymbol{H}}$ can be expressed as

$$\begin{aligned} \underline{\boldsymbol{\Xi}} &= \boldsymbol{F}_N \underline{\boldsymbol{H}} \boldsymbol{F}_M^H \\ &= [\boldsymbol{\Xi}_1, \cdots, \boldsymbol{\Xi}_m, \cdots, \boldsymbol{\Xi}_M] \end{aligned} \tag{39}$$

with its component diagonal sub-matrices being

$$\boldsymbol{\Xi}_m = [\boldsymbol{\Xi}_{1,m}, \cdots, \boldsymbol{\Xi}_{n,m} \cdots, \boldsymbol{\Xi}_{N,m}]^T. \tag{40}$$